



RESEARCH MEMORANDUM

DESIGN AND EVALUATION OF A TURBOJET EXHAUST SIMULATOR,
UTILIZING A SOLID-PROPELLANT ROCKET MOTOR, FOR USE
IN FREE-FLIGHT AERODYNAMIC RESEARCH MODELS

By Carlos A. de Moraes, William K. Hagginbothom, Jr.,
and Ralph A. Falanga

Langley Aeronautical Laboratory
Langley Field, Va.

**NATIONAL ADVISORY COMMITTEE
FOR AERONAUTICS
WASHINGTON**

December 17, 1954
Declassified September 13, 1957

NATIONAL ADVISORY COMMITTEE FOR AERONAUTICS

RESEARCH MEMORANDUM

DESIGN AND EVALUATION OF A TURBOJET EXHAUST SIMULATOR,
UTILIZING A SOLID-PROPELLANT ROCKET MOTOR, FOR USE
IN FREE-FLIGHT AERODYNAMIC RESEARCH MODELSBy Carlos A. de Moraes, William K. Hagginbothom, Jr.,
and Ralph A. Falanga

SUMMARY

A method has been developed for modifying a rocket motor so that its exhaust characteristics simulate those of a turbojet engine. The analysis necessary to the design is presented along with tests from which the designs are evaluated. Simulation was found to be best if the exhaust characteristics to be duplicated were those of a turbojet engine at high altitudes and with the afterburner operative.

INTRODUCTION

Propulsive jets issuing from turbojet engines that power our present-day high-speed aircraft can have an appreciable interference effect on the external aerodynamics of aircraft configurations. Some effects of propulsive jets on base and boattail pressure drags, on wing or tail surfaces located in the immediate vicinity of the jet, and on configuration trim characteristics have been reported in previous research work and may be found in references 1 to 3.

The Langley Pilotless Aircraft Research Division has been conducting an investigation of propulsive jet interference effects on aerodynamic research models designed to simulate turbojet-powered aircraft. In order to be able to evaluate jet interference on research models, it was necessary to devise a means of simulating the turbojet exhaust characteristics.

Inasmuch as it is standard practice at PARD to use solid-propellant rocket motors to propel free-flight models, there is considerable advantage to be gained by adapting these motors to provide turbojet exhaust simulation as well as propulsion.

As rocket motors operate at much higher total pressures than turbojet exhaust total pressures, a means of throttling the rocket total pressures had to be developed. The temperature of the rocket exhaust and temperature of turbojet exhaust with afterburner on are close enough to present no problem here.

This report advances a technique for analyzing, proportioning, and a means of simulating the essential turbojet exhaust characteristics. These essential characteristics are expressed in the parameters jet thrust, jet weight flow, and jet total pressure ratios, and are γ_j/γ_o , p_j/p_o , M_j/M_o , and $\sqrt{R_o t_o/R_j t_j}$.

Five turbojet simulators with different requirements have been designed and successfully tested. The results are compared herein with the initial design values. Static testing necessary to evaluate performance of these five units was conducted at the Langley rocket test cell.

SYMBOLS

A	area, in. ²
c	propellant burning rate coefficient
C _F	thrust coefficient, $F_j/q_o A_o$
f/a	fuel air ratio
F	thrust, lb
F _n	net thrust, lb
g	acceleration due to gravity, 32.2 ft/sec ²
H	total pressure, lb/sq in. abs
M	Mach number
n	propellant burning rate exponent
p	static pressure, lb/sq in. abs
q	dynamic pressure, $\frac{\gamma p M^2}{2}$, lb/sq in. abs

r	rocket propellant burning rate, in./sec
R	gas constant, $\frac{\text{ft-lb}}{\text{lb-}^\circ\text{R}}$
S	rocket propellant burning surface, in. ²
t	static temperature, $^\circ\text{R}$
T	total temperature, $^\circ\text{R}$
v	velocity, ft/sec
\dot{w}	weight flow, lb/sec
γ	ratio of specific heats, c_p/c_v
ρ	density, lb/in. ³

Subscripts:

c	rocket combustion chamber
j	jet exit
o	free stream
t	rocket throat

ANALYSIS AND DESIGN

The primary parameters to be considered in the design of a turbojet simulator are the jet thrust, the jet weight flow relative to the free-stream weight flow, and the jet total pressure relative to the free-stream static pressure. Consideration of these parameters is necessarily based upon the turbojet operating and altitude characteristics to be simulated and the scale to be used. In general, the simulator will not be used at the same altitude as the full-scale turbojet. Thus, the simulator requirements are obtained by proportioning the full-scale engine characteristics according to the differences in altitude and size.

Simulation of the jet thrust is obtained from the jet thrust coefficient, defined by

$$C_{Fj} = \frac{F_j}{q_o A_o} \quad (1)$$

where

$$F_j = \frac{\dot{w}_j}{g} v_j + (p_j - p_o) A_j \quad (2)$$

or

$$F_j = A_j \left[p_j (1 + \gamma_j M_j^2) - p_o \right] \quad (2a)$$

and

$$q_o = \frac{\gamma_o p_o M_o^2}{2} \quad (3)$$

Substituting equations (2a) and (3) into equation (1) yields

$$C_{Fj} = 2 \frac{A_j}{A_o} \left[\frac{\frac{p_j}{p_o} (\gamma_j M_j^2 + 1) - 1}{\gamma_o M_o^2} \right] \quad (4)$$

Thus, if the scale model is to be tested at the same Mach number as the full-scale configuration, simulation of the thrust then depends solely on the duplication of propulsive jet ratio of specific heats γ_j , the jet static-pressure ratio p_j/p_o , and the jet Mach number M_j .

Simulation of the weight flow characteristics is obtained from the ratio of the jet weight flow to a representative free-stream weight flow. In equation form, this ratio is R_t

$$\frac{\dot{w}_j}{\dot{w}_o} = \frac{(\rho A v)_j}{(\rho A v)_o} \quad A_j \text{ is free area}$$

or

$$\frac{\dot{w}_j}{\dot{w}_o} = \frac{\gamma_j p_j}{\gamma_o p_o} \left(\frac{M_j}{M_o} \right)^2 \frac{A_j}{A_o} \frac{v_o}{v_j} \quad (5)$$

Simulation of the jet weight flow characteristics is then subject to the same parameters as the thrust, with the addition of the free stream to jet velocity ratio. The additional requirement that this condition imposes is that $(R_t)_j$ be proportional to the full-scale engine; that is,

$$\frac{v_o}{v_j} \sim \sqrt{\frac{R_o t_o}{R_j t_j}} \quad (6)$$

The criteria of jet total-pressure ratio (H_j/p_o) raises no new requirements as the jet Mach number and ratio of specific heats, and the jet static-pressure ratio (p_j/p_o) are already requirements for simulation.

Thus, use of a small rocket motor operating to simulate a full-scale turbojet engine depends upon obtaining exhaust parameters γ_j/γ_o , p_j/p_o , M_j/M_o , and $\sqrt{R_o t_o/R_j t_j}$ equal to those of the full-scale turbojet exhaust, if the flight Mach number of the rocket motor is the same as that of the turbojet engine.

Characteristically, a rocket motor operates at a high total pressure and with a small throat relative to a turbojet engine. The exhaust gas temperature is also higher but is close enough to an afterburner exhaust to be lived with as the free-stream temperature at its lower test altitude is higher than that of the full-scale turbojet. The ratio of specific heats and the gas constant for the two exhausts will also vary some, depending on the particular propellant to be used. The main requirement then is to dissipate the high pressure of the rocket exhaust and increase its choking area. Both of these aims may be accomplished by exhausting the rocket gases through a double-throat nozzle instead of the usual single throat.

As may be gathered from the above discussion, closest simulation of the turbojet exhaust characteristics occurs for a turbojet operating with afterburner on at high altitudes.

Design of the rocket motor and simulator is then accomplished by the simultaneous solution of the rocket ballistic and one-dimensional channel flow equations. The weight flow from the rocket motor operating at equilibrium conditions is given by

$$\dot{w} = r S \rho \quad (7)$$

where

$$r = c H_c^n \quad (8)$$

Thus,

$$\dot{w} = c H_c^n S \rho \quad (9)$$

Choice of a rocket motor, either as manufactured or modified to meet space requirements, fixes all the parameters except combustion chamber pressure. Thus, the combustion chamber pressure necessary to produce the required weight flow is given by

26.8

$$H_c = \left(\frac{\dot{w}}{cS\rho} \right)^{1/n} \quad (9a)$$

The throat area necessary to produce the required combustion chamber pressure and still yield the desired jet total pressure and exit area may be obtained from considering the conservation of mass between the two choking areas.

$$(\rho Av)_t = (\rho Av)_j$$

or

$$\left(\frac{\gamma p M^2 A}{v} \right)_t = \left(\frac{\gamma p M^2 A}{v} \right)_j \quad (10)$$

Inasmuch as it was assumed that there was no heat transfer to the simulator walls and because $M_j = M_t = 1.0$,

$$\gamma_t = \gamma_j \quad \text{and} \quad v_j = v_t$$

thus, equation (10) becomes

$$A_t = \frac{p_j}{p_t} A_j$$

or

$$A_t = \left(\frac{H_j}{H_c} \right) A_j \quad (11)$$

where

$$H_c = H_t$$

The physical dimensions of the plenum chamber may be determined from a one-dimensional flow analysis between the choking stations. If a normal shock is assumed to stand in the plenum chamber, the Mach number necessary to give the desired total-pressure loss and hence the area necessary to give the needed Mach number are easily obtained. In practice, it was found that this was the minimum area needed and that better results were obtained if the actual area was at least 10 percent larger than that computed.

Analysis of the flow downstream of the normal shock is accomplished from the continuity equation and the assumption of no heat loss in the jet. From equation (10)

$$M_x^2 = \left(\frac{p_t A_t}{p_x A_x} \frac{v_x}{v_t} \right) M_t^2$$

where

$$v = M \sqrt{\gamma g R t}$$

$$M_t = 1.00$$

and x is any station in the simulator downstream of the normal shock. Therefore,

$$\left(M_x \right)^2 = \left(\frac{p_t A_t}{p_x A_x} \right)^2 \frac{t_x}{t_t}$$

If no heat loss is assumed,

$$\frac{t_x}{t_t} = \frac{1}{\frac{2}{\gamma + 1} \left(1 + \frac{\gamma - 1}{2} M_x^2 \right)}$$

so that

$$M_x^4 + \frac{2}{\gamma - 1} M_x^2 - \frac{\gamma + 1}{\gamma - 1} \left(\frac{p_t A_t}{p_x A_x} \right)^2 = 0$$

or

$$M_x = \left[\frac{1}{1 - \gamma} + \frac{1}{2} \sqrt{\left(\frac{2}{\gamma - 1} \right)^2 + 4 \frac{\gamma + 1}{\gamma - 1} \left(\frac{p_t A_t}{p_x A_x} \right)^2} \right]^{1/2} \quad (12)$$

The static pressure at the throat p_t is computed from the measured combustion chamber pressure whereas p_x is measured directly. Thus, the Mach number and hence the total pressure may be determined at any station downstream of the normal shock where a static-pressure measurement is made. Flow parameters at the exit may be determined from measurements upstream of the exit and a one-dimensional flow analysis.

APPARATUS AND TESTS

A typical turbojet simulator of the type tested is shown in figure 1. It consists essentially of a combustion chamber, a flow control nozzle, a plenum chamber, and a convergent exit section. The basic simulator tested utilized a modified 3.25-inch aircraft rocket combustion chamber containing a specially machined cordite SU/K propellant grain. Dimensions of the grain, as well as those of duct cross-sectional area at the nozzle throat and jet exit, were altered somewhat for different tests to meet different simulation requirements.

Another simulator tested utilized modified JPN propellant.

The simulator tests were conducted at the Langley rocket test cell. The test setup employed is illustrated in figure 2 which shows a typical simulator mounted on a thrust stand and instrumented for the measurement of pressures at the combustion chamber, plenum chamber, and along the convergent exit section.

The thrust stand functions in such a manner that the deflection of a beam proportional to the thrust exerted is measured by electrical strain gages and recorded on a recording galvanometer. Pressures are similarly measured and recorded by using electrical pressure transmitters. A timer incorporated in the recording system provides a time history of thrust and pressure measurements.

RESULTS AND DISCUSSION

The details of design of a typical turbojet simulator are presented in the appendix. Two important constants necessary to the ballistic design of the rocket motor are the burning rate coefficient c and the burning rate exponent n . At the time of these tests, the available data on these two constants were limited and were not consistent to the accuracy desired in the present tests. Hence, part of the development tests were undertaken for the purpose of determining these constants over the desired pressure range and to the desired accuracy.

The burning rate is given by equation (8) as

$$r = cH_c^n \quad (8)$$

or

$$\log_e r = \log_e c + n \log_e H_c$$

which is a linear equation of slope n and with $\log_e c$ as an intercept. The data obtained from the present development tests are presented in this form in figure 3. The range of these data is small as it only covers the range of combustion chamber pressures desired in the present tests. Because of this small range, the data may not be applicable if extrapolated. Hence, no attempt was made to evaluate the burning rate coefficient c . Rather, the burning rates necessary to the design of the turbojet simulator were obtained directly from the data in figure 3.

Since this work was done, reference 4 has been published containing data similar to that of figure 3 although much more extensive in nature. The burning rate exponent n of the present tests (0.56) agrees well with that of the reference tests (0.54), although the burning rate coefficient is considerably different and results in higher burning rates at a given combustion chamber pressure. This effect may be due to the fact that in the reference tests the grain was end burning whereas it was radial burning in the present tests. Thus, the erosion effects on the grain and the heat transfer would be considerably different.

As presented above, the design is a straightforward proposition and close simulation will always be attained. However, in practice this may not always be the case as it is possible to have a combination of parameters that cannot be satisfied by the particular rocket characteristics (for instance, the computed chamber pressure may be such that chuffing, that is, sporadic burning may result). In general though, it is possible to redesign the rocket motor to eliminate any such features and still simulate the desired turbojet exhaust characteristics to within the limits of this report.

In the present case, a turbojet engine operating at a free-stream Mach number of 1.3 and at an altitude of 35,000 feet is to be simulated with a 1/10-scale model operating at a free-stream Mach number of 1.3 and at an altitude of 3,000 feet. Results of the static firing of this simulator are presented in figure 4. As may be seen, the measured values of thrust, weight flow, and total pressure are very close to the design values. A comparison of the design and average test values is given in the following table:

Quantity	Design	Average test	Average deviation, percent	Maximum deviation, percent
\dot{w}_j , lb/sec	4.64	4.58	1.6	4.5
H_j , lb/sq in. abs	73.8	72.2	2.1	6.0
F_j , lb	620	606	2.2	6.5

The average test value in this case is not the usual one in rocket test work, that is, the average value over the entire burning time of 1.67 seconds. Rather, it is defined as the average value after the initial ignition surge and before the tail-off at burnout. This definition is used because it is not the overall rocket performance that is of interest but rather the ability to obtain the desired average exhaust characteristics over a period of time. Hence, in this case, the average quantity value is taken from 0.1 second to 1.56 seconds. The average deviations between the design and test values were small whereas the maximum deviation was of the order of three times as large. Inasmuch as turbojet characteristics are themselves somewhat nebulous unless obtained from tests, the differences involved are no cause for concern.

Presented in figure 5 are typical plots of the pressure and Mach number variations downstream of the plenum chamber. The static pressures were measured at the indicated orifices whereas the Mach number and total-pressure variations were determined as described previously. Although no measurements were made at the exit, the total pressure was computed from equation (11) and the Mach number was determined from that at E by correcting for the differences in area. It was then possible to compute the static pressure at the exit. The agreement between the total pressure at E and at the exit, and the fact that the thrust computed from the exit conditions reproduced the measured thrust well (fig. 6) lends credulity to the assumptions made in determining the exit conditions. This result was undoubtedly due to the short burning time of the rocket grain in the present tests. If larger units, having longer burning times, were to be used the temperature loss of heat would become appreciable and would have to be corrected for in equation (11).

It is evident from the resultant total-pressure variation that the flow in the turbojet simulator is not as assumed, except near the exit. Some distance is required to straighten out the flow after the throttling process and this process is undoubtedly accomplished over some distance rather than at one point, as assumed. Inasmuch as some of the assumptions made in the analysis are apparently invalid except near the exit, the exit conditions, and hence the thrust, may be computed in a flight model by measuring either the combustion chamber pressure or a static pressure near the exit of the simulator, preferably the latter.

Other simulators have been designed by the procedure outlined previously. Results from tests of these installations are given in figure 7 and in the table on following page.

Model 1; solid propellant, cordite SU/K				
Quantity	Design value	Average test value	Average deviation, percent	Maximum deviation, percent
F_j	546	534	2.3	6.5
H_j	68.3	67.1	1.7	5.2
\dot{w}_j	3.88	3.98	2.5	5.2
Model 2; solid propellant, cordite SU/K				
F_j	703	687	2.2	6.4
H_j	83.9	82.3	1.9	3.4
\dot{w}_j	5.34	5.20	2.6	4.0
Model 3; solid propellant, cordite SU/K				
F_j	510	522	2.3	6.0
H_j	74.4	72.7	2.1	4.7
\dot{w}_j	3.93	3.98	1.3	2.6
Model 4; solid propellant, JPN				
F_j	334	349	4.4	11.2
H_j	115	108.6	5.5	10.4
\dot{w}_j	1.95	2.04	4.7	7.8

The first three simulators listed in the table were designed around the same rocket motor used in the illustrative example discussed previously. The differences between the design and the average test values are all very similar and satisfactory. The fourth model listed, however, was designed around a 3.25-inch aircraft rocket motor. This motor has a JPN propellant grain molded in a cruciform configuration. It is not as consistent in performance or as easy to modify as is the cordite grain. Although the maximum deviations in the latter case are large, the full-scale turbojet characteristics being simulated are, in general, computed values rather than test values; hence, they are probably not of any greater accuracy than the worst simulator results.

An effort was made to produce a shorter simulator and hence decrease the weight. However, apparently because the flow never did completely fill the channel, the thrust was very unsteady in nature and

the exit was supersonic. In order to remedy this situation, a small plate was welded in the plenum chamber normal to the center line. The flow from the throat impinged on this plate and produced a strong shock which resulted in a stable flow in the convergent channel with sonic flow at the exit. This shorter simulator would be beneficial in a body with a highly convergent or no afterbody. For most cases, however, the models have high-fineness-ratio afterbodies and hence the original design has been used more extensively.

Although solid-propellant rocket motors were used exclusively in the present tests, this technique of simulating turbojet exhausts can be applied to any installation where the desired jet total pressure is appreciably lower than the combustion or reaction chamber pressure.

The impression may have been given that the design of a turbojet simulator from the ballistic data given in this report will automatically yield results within the limits stated previously. Actually, any design should be verified experimentally as some slight changes may be advantageous. If the particular installation is significantly different physically from that of the present tests, development tests may be necessary to obtain the same accuracy as was obtained in the present tests.

CONCLUSION

It has been demonstrated that a rocket motor can be modified to simulate satisfactorily the exhaust characteristics of a turbojet engine for use in free-flight aerodynamic research models. Simulation was found to be best if the exhaust characteristics to be duplicated were those of a turbojet engine at high altitudes and with the afterburner operative.

Langley Aeronautical Laboratory,
National Advisory Committee for Aeronautics,
Langley Field, Va., September 7, 1954.

APPENDIX

ILLUSTRATION OF DESIGN PROCEDURE

In order to illustrate the design procedure, suppose it were desired to simulate a turbojet engine operating at a free-stream Mach number of 1.30 and at an altitude of 35,000 feet. The operating characteristics of such an engine might be as follows:

$$\begin{aligned}
 F_n &= 11,200 \text{ lb} && \text{net thrust put out from engine when installed in nacelle} \\
 \dot{w}_a &= 130 \text{ lb/sec} \\
 H_j/p_o &= 5.60 \\
 A_j &= 785 \text{ in.}^2 \\
 f/a &= 0.065 \\
 T_j &= 3200^\circ \text{ R} \\
 \gamma_j &= 1.27
 \end{aligned}$$

The jet thrust coefficient is given by

$$C_F = \frac{F_j}{q_o A_o}$$

where

$$F_j = F_n + \frac{\dot{w}_j}{g} v_o = 11,200 + \frac{(130)(1265)}{32.2}$$

or

$$F_j = 16,310 \text{ lb}$$

and A_o is a representative area. In this case the simulator is to be a 1/10-scale model operating at a free-stream Mach number of 1.3 and at an altitude of 3,000 feet. Equating the thrust coefficient of the model and full-scale configuration yields

$$(C_F)_{TJ} = (C_F)_R$$

or

$$\left(\frac{F_j}{.7 p_o M_o^2 A_o} \right)_{TJ} = \left(\frac{F_j}{.7 p_o M_o^2 A_o} \right)_R \quad (F_j)_R = (.7 p_o M_o^2 A_o)_R$$

where TJ refers to the full-scale turbojet engine and R refers to the rocket model. Inasmuch as $(M_o)_{TJ} = (M_o)_R$, $A_{TJ} = 100A_R$ and the altitude pressure ratio is

$$\frac{P_{3,000}}{P_{35,000}} = 3.81$$

$$(F_j)_R = \frac{(16,310)(3.81)}{100} = 620 \text{ lb}$$

Equating the weight flow ratios yields

$$\left(\frac{\dot{w}_j}{\dot{w}_o} \right)_{TJ} = \left(\frac{\dot{w}_j}{\dot{w}_o} \right)_R$$

or

$$\left(\frac{\dot{w}_j}{\gamma_o P_o M_o^2 A_o} \right)_{TJ} = \left(\frac{\dot{w}_j}{\gamma_o P_o M_o^2 A_o} \right)_R$$

where

$$(\dot{w}_j)_{TJ} = (\dot{w}_a) (1 + f/a) = 138.6 \text{ lb/sec}$$

$$(M_o)_{TJ} = (M_o)_R$$

$$(A_o)_{TJ} = 100(A_o)_R$$

$$\frac{(v_o)_{TJ}}{(v_o)_R} = \frac{1265}{1434} = 0.882$$

Therefore

$$(\dot{w}_j)_R = \frac{(138.6)(3.81)(0.882)}{100} = 4.64 \text{ lb/sec}$$

$$(H_j)_R = (5.60)(13.18) = 73.80 \text{ lb/sq in. abs}$$

and

$$A_j = 7.85 \text{ in.}^2$$

These then are the rocket requirements if it is to simulate the given turbojet exhaust characteristics.

The rocket propellant used in most of this work was British cordite SU/K propellant. It was chosen principally because of the ease with which it may be modified. In this particular case, the propellant was modified to meet space requirements by reducing the outer diameter from 4.30 to 2.50 inches and the length from 32.25 to 29.7 inches. The resultant grain burning surface was then 308 inches².

The combustion chamber pressure necessary to produce the desired weight flow is obtained from equation (7) and figure 3. The burning rate is given by

$$r = \frac{\dot{w}}{S\rho} \quad (7)$$

where

$$\dot{w} = 4.64 \text{ lb/sec}$$

$$S = 308 \text{ in.}^2$$

and

$$\rho = 0.057 \text{ lb/in.}^3$$

Thus,

$$r = \frac{4.64}{308 \times 0.057} = 0.264 \text{ in./sec}$$

The combustion chamber obtained from figure 3 is then 400 pounds per square inch gage, or at the design altitude of 3,000 feet

$$H_c = 413 \text{ lb/sq in. abs}$$

The area of the throat is given by

$$A_t = \frac{H_j A_j}{H_c} = \frac{(73.7)(7.85)}{413} = 1.405 \text{ in.}^2$$

The area in the plenum chamber, needed to hold a normal shock, is obtained by assuming one-dimensional isentropic flow on either side of the normal shock. The change in total pressure across a normal shock is given by

$$\frac{H_1}{H_2} = \left(\frac{2\gamma}{\gamma+1} M_1^2 - \frac{\gamma-1}{\gamma+1} \right)^{\frac{1}{\gamma-1}} \left[\frac{(\gamma-1) M_1^2 + 2}{(\gamma+1) M_1^2} \right]^{\frac{\gamma}{\gamma-1}}$$

where $H_1 = H_c$ and $H_2 = H_j$. As the gas generated from burning this particular propellant has a ratio of specific heats of 1.25, the Mach number in the plenum chamber, ahead of the normal shock, needed to obtain the required pressure change H_c/H_j is

$$M_1 = 3.32$$

The area necessary to produce this Mach number is given by

$$\frac{A^*}{A_1} = M_1 \left(\frac{\frac{\gamma+1}{2}}{1 + \frac{\gamma-1}{2} M_1^2} \right)^{\frac{\gamma+1}{2(\gamma-1)}}$$

where

$$A^* = A_t$$

Thus,

$$A_1 = 12.32 \text{ in.}^2$$

$$d_1 = 3.96 \text{ in.}$$

The diameter was then arbitrarily increased to 4.50 inches to insure stable flow at the exit.

REFERENCES

1. de Moraes, Carlos A., and Nowitsky, Albin M.: Experimental Effects of Propulsive Jets and Afterbody Configurations on the Zero-Lift Drag of Bodies of Revolution at a Mach Number of 1.59. NACA RM L54C16, 1954.
2. Cortright, Edgar M., Jr., and Schroeder, Albert H.: Investigation at Mach Number 1.91 of Side and Base Pressure Distributions Over Conical Boattails Without and With Jet Flow Issuing From Base. NACA RM E51F26, 1951.
3. Bressette, Walter E.: Investigation of the Jet Effects on a Flat Surface Downstream of the Exit of a Simulated Turbojet Nacelle at a Free-Stream Mach Number of 2.02. NACA RM L54E05a, 1954.
4. Hirst, R., and Ellis, W. R.: A Laboratory Method of Studying the Combustion of Cordite. Tech. Note No. R.P.D. 96, British R.A.E., Feb. 1954.

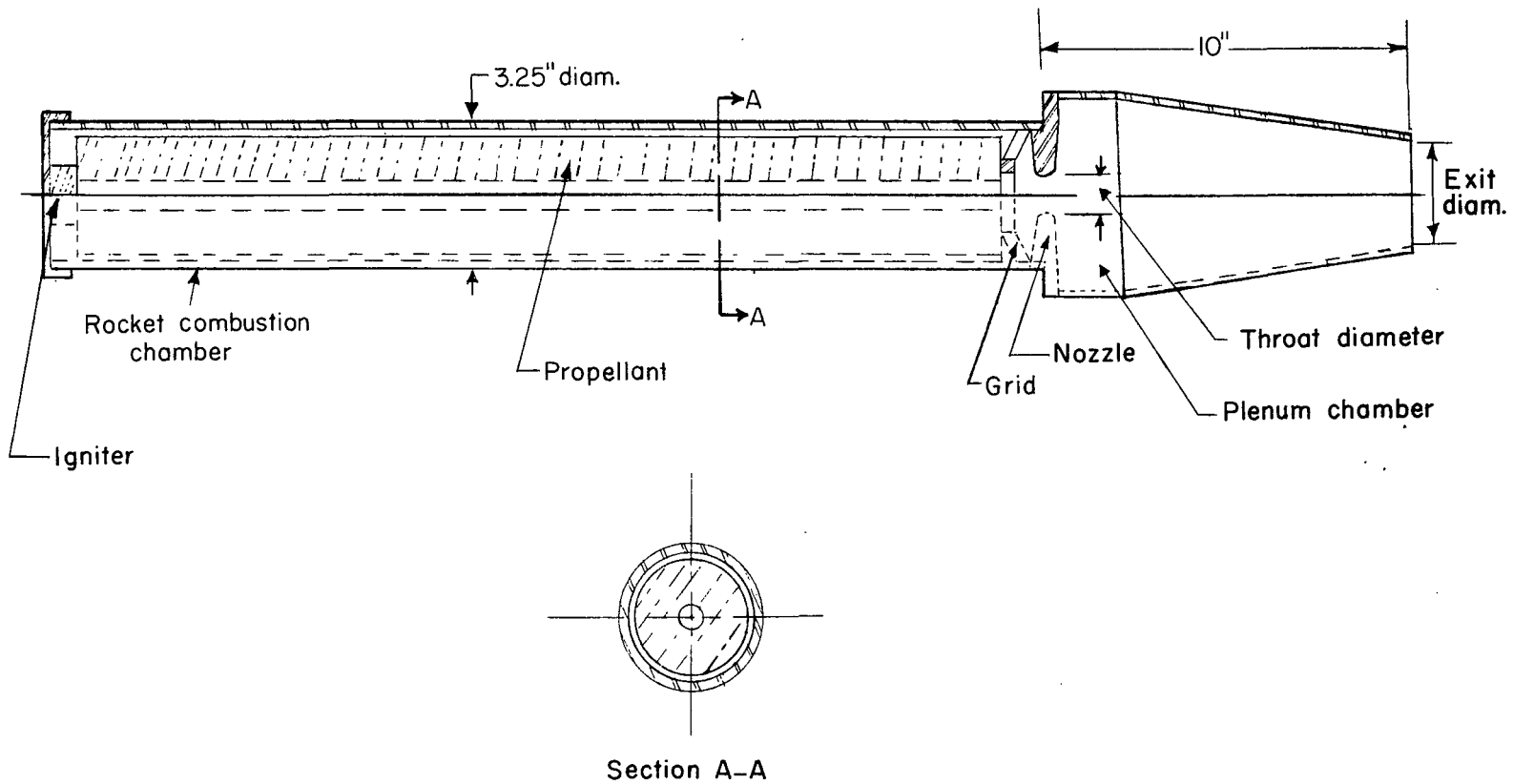
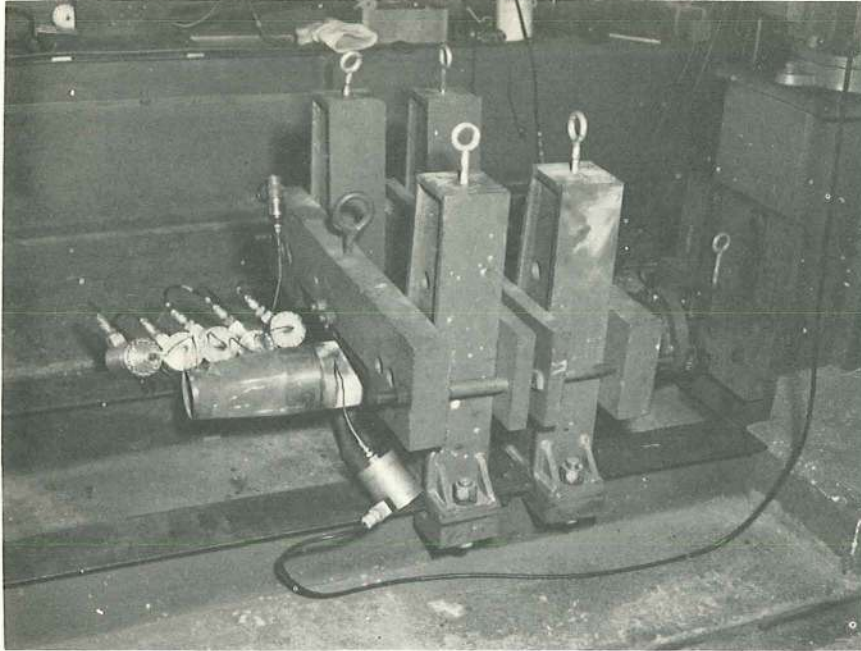
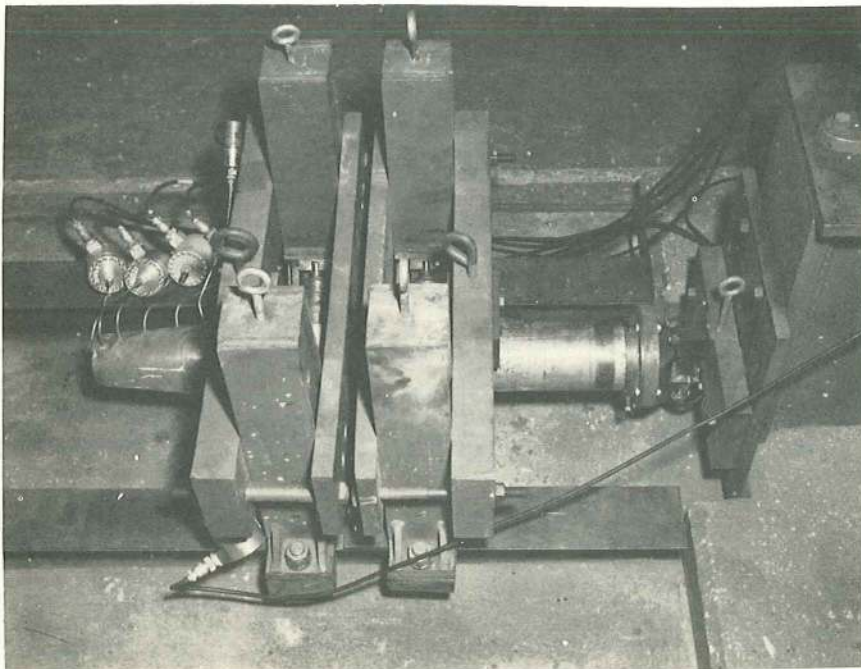


Figure 1.- Cross section of typical turbojet simulator.



L-84932



L-84933

Figure 2.- Photographs of typical test setup.

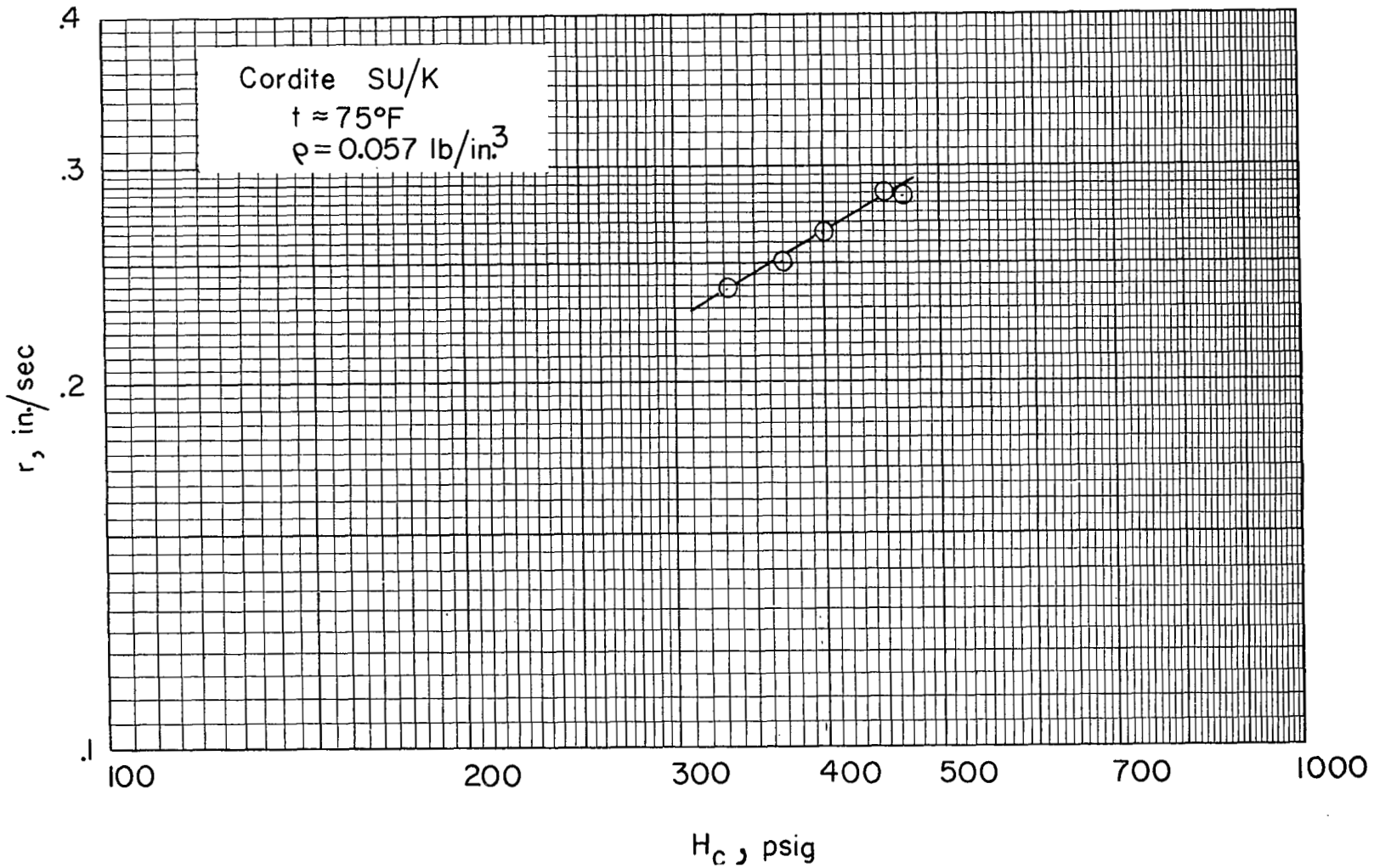


Figure 3.- Burning rate as a function of combustion chamber pressure.

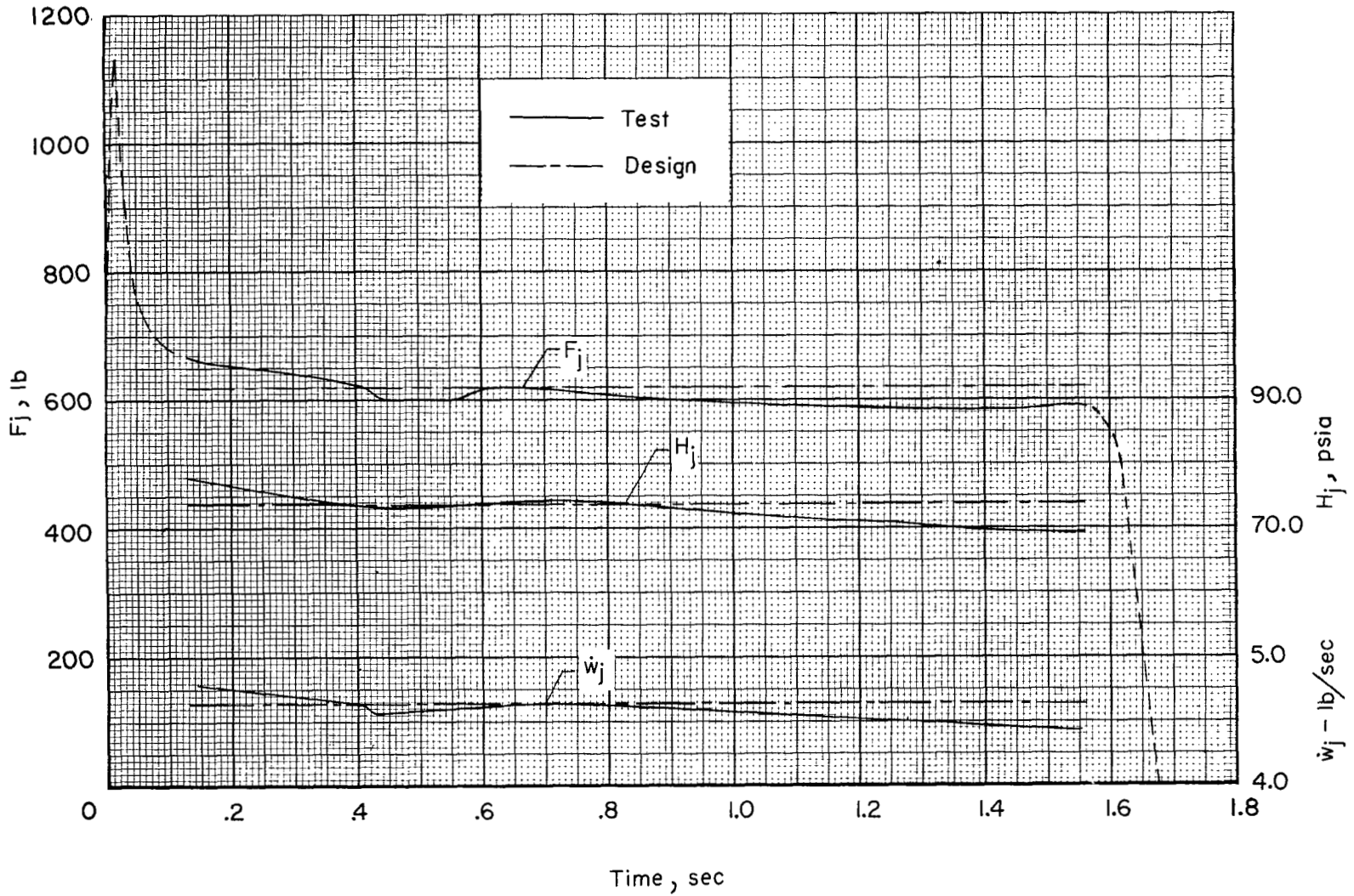


Figure 4.- Comparison between design and test values of flow parameters.

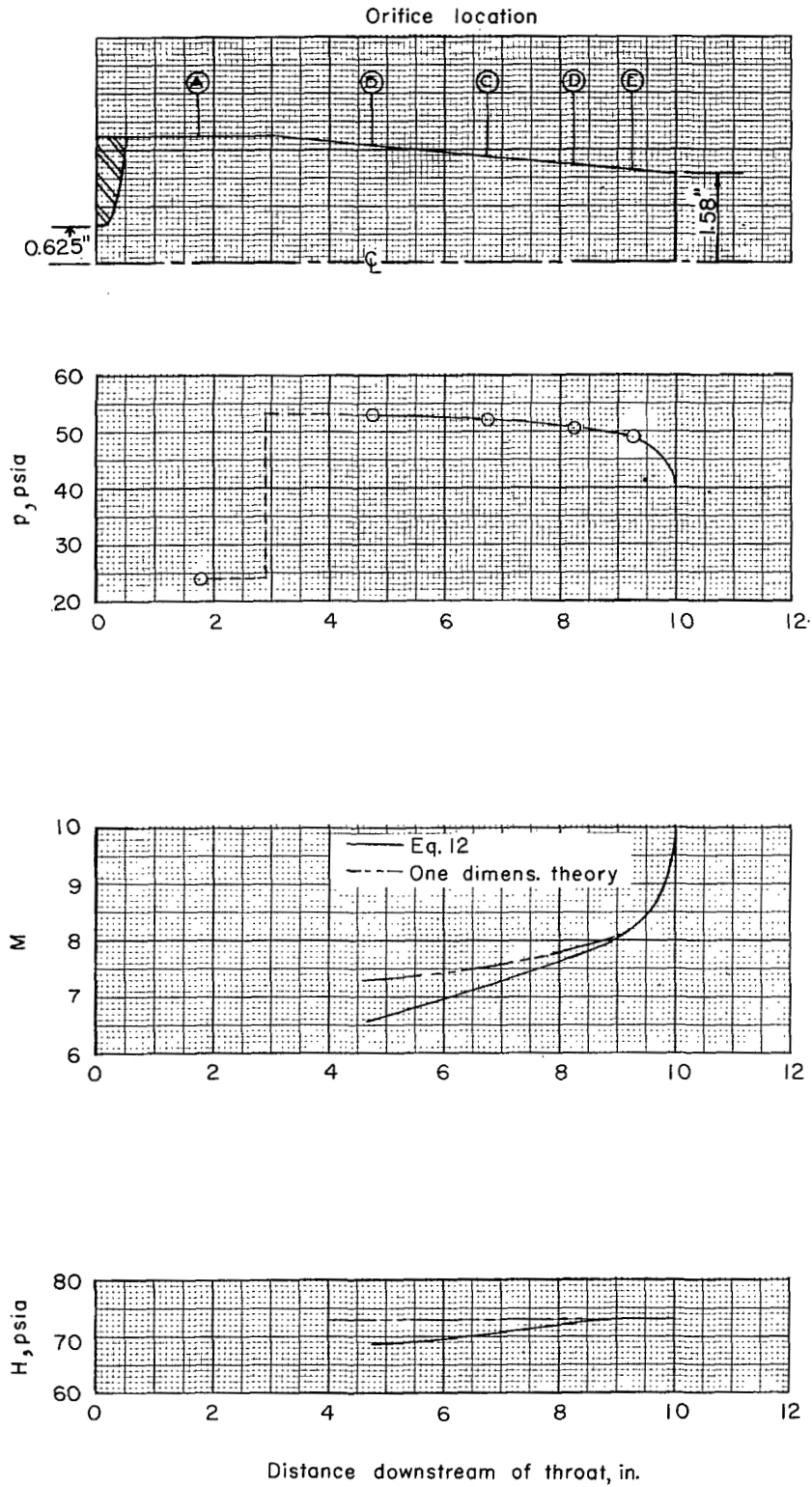


Figure 5.- Variation of pressure and Mach number in turbojet simulator.

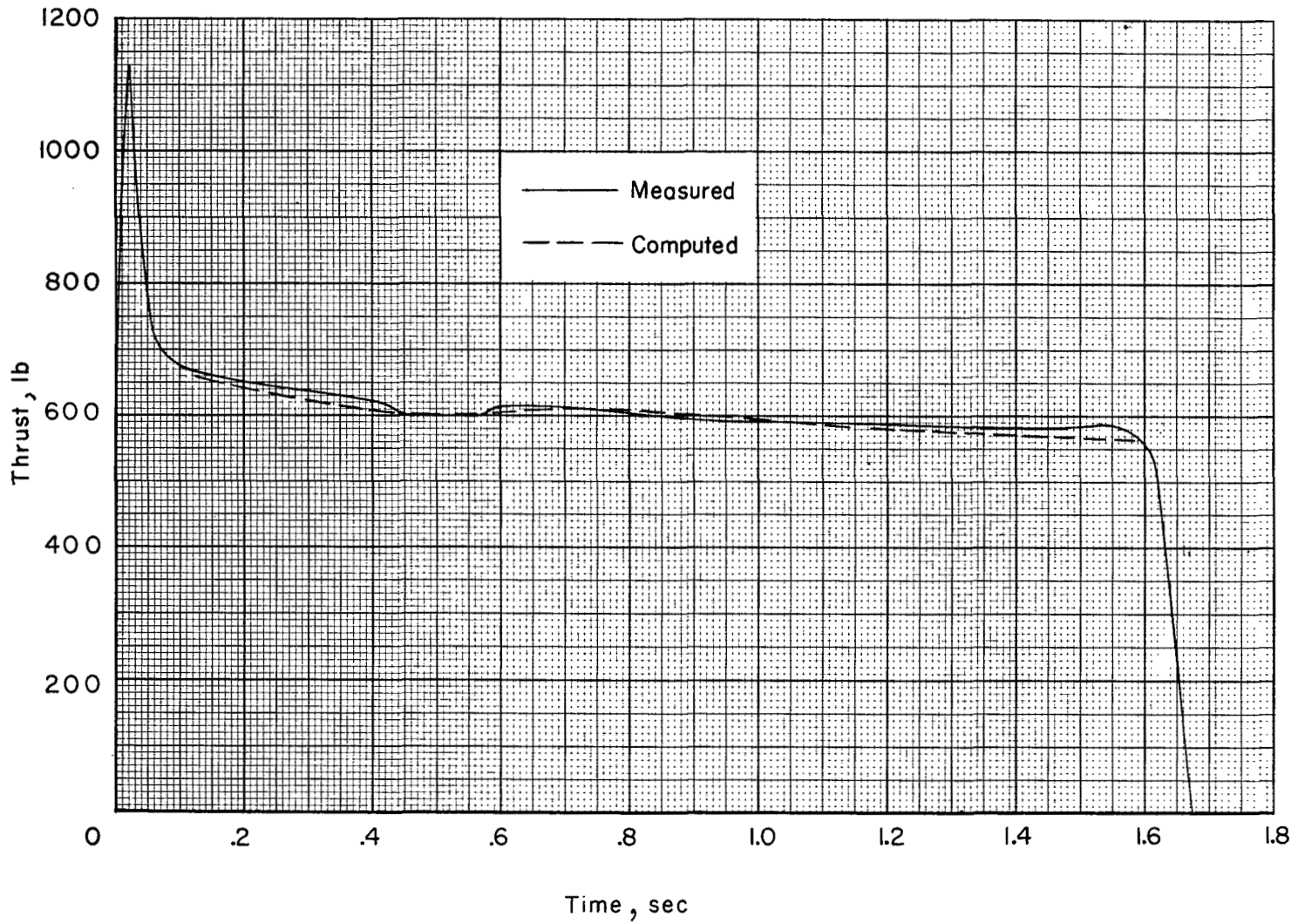


Figure 6.- Comparison between measured and computed thrust.

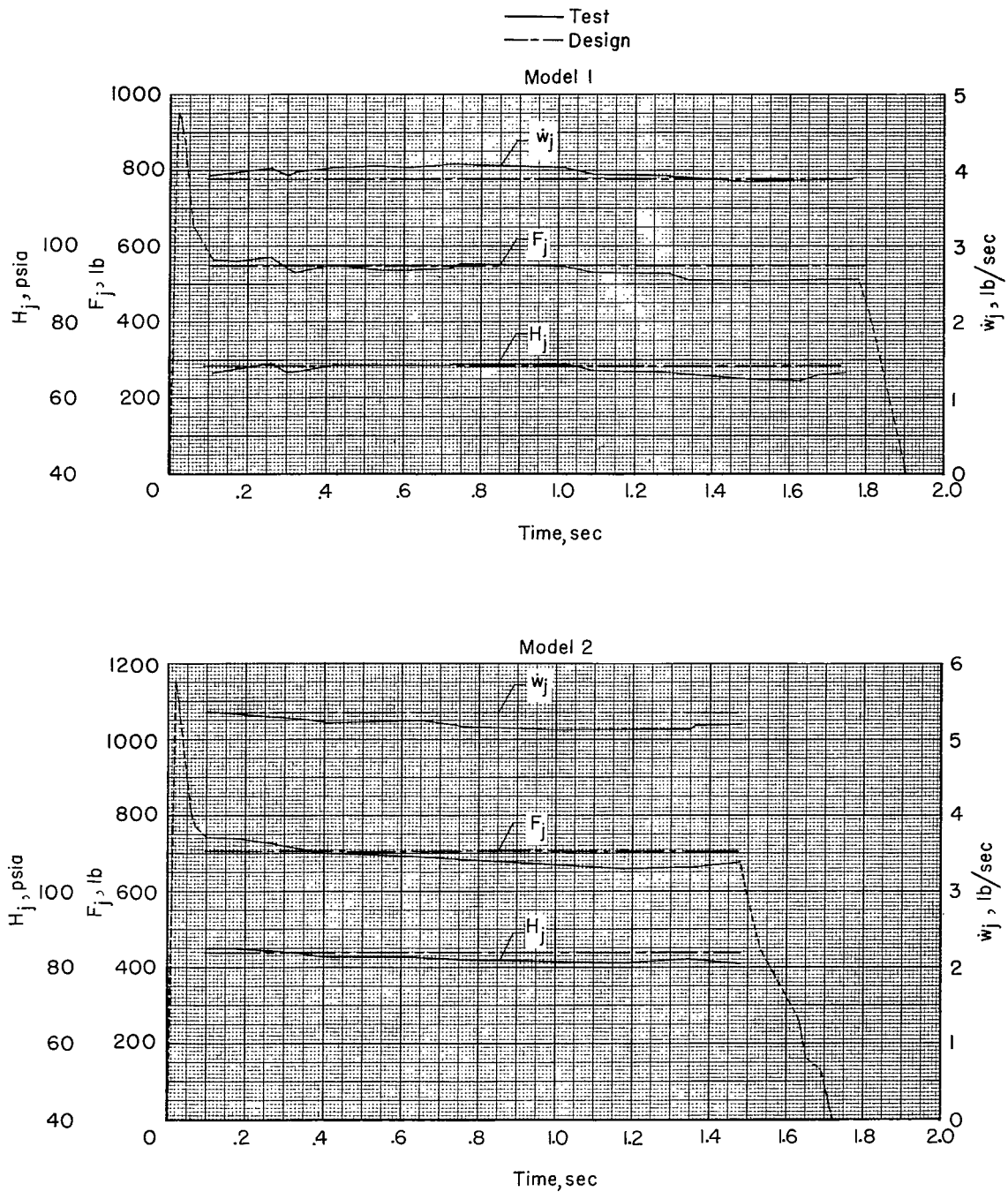


Figure 7.- Comparison between design and test flow parameters in turbojet simulators.

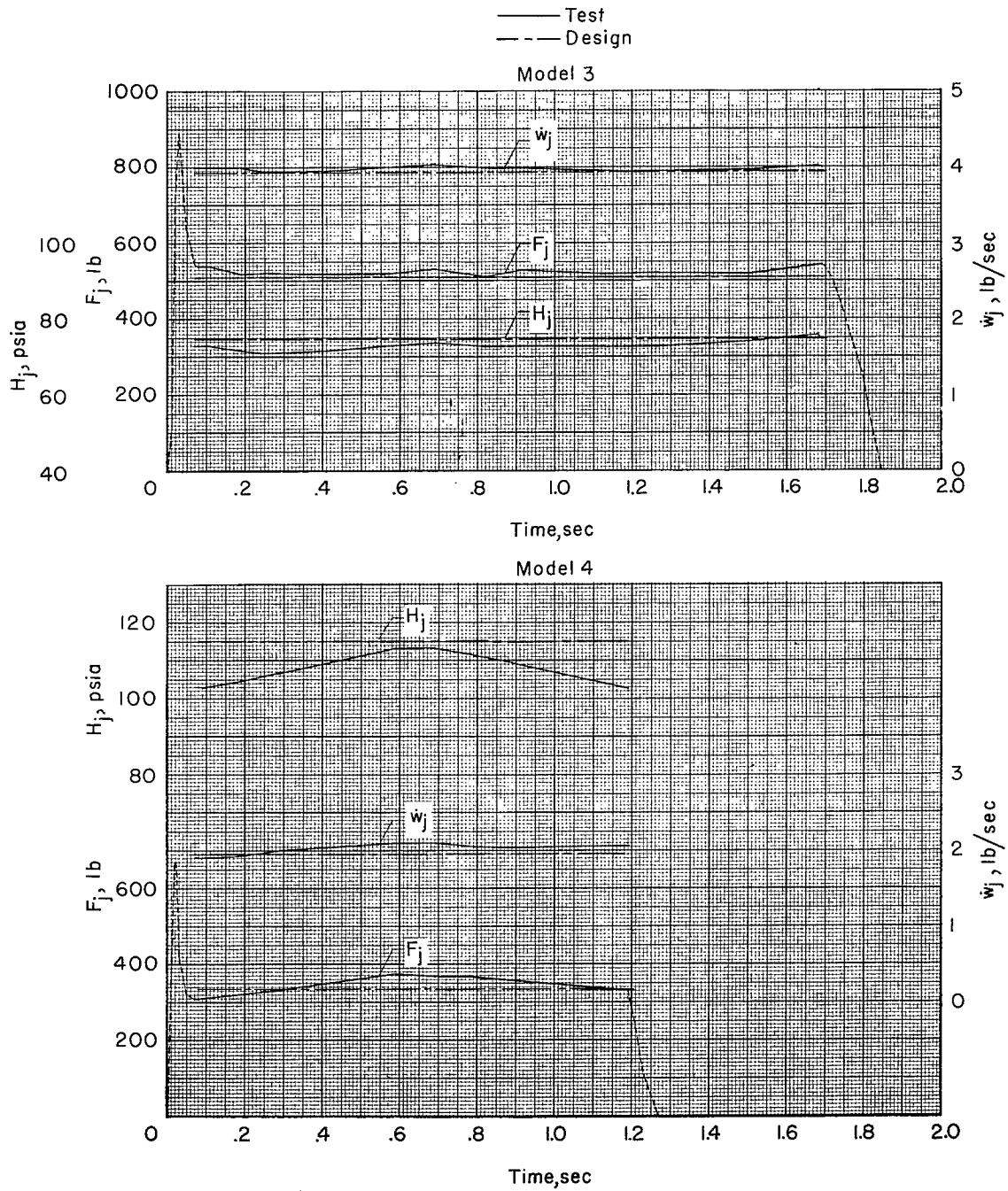


Figure 7.- Concluded.

11/21/57



NASA Technical Library



3 1176 01437 1778

